Displacement Uncertainty in Interferometric Radius Measurements

T. L. Schmitz[1], C. J. Evans[2] (1), A. Davies[3], W. T. Estler[1] (2)
[1]National Institute of Standards and Technology (NIST), Gaithersburg, MD, USA
[2]Zygo Corporation, Middlefield, CT, USA
[3]University of North Carolina at Charlotte, Charlotte, NC, USA

Abstract
Interferometric radius measurements may be completed using a radius bench, where radius is defined as the displacement between the confocal and cat's eye nulls (identified using a figure measuring interferometer). Measurements of a Zerodur sphere have been completed on the X-ray Optics Calibration interferometer (XCALIBIR) and a coordinate measuring machine. Larger recorded disagreements than indicated by the current uncertainty analysis call for an exploration of the analysis model. This paper details uncertainties associated with the use of multiple displacement measuring interferometers (DMIs) to record motion in a single axis by treating the specific case of displacement measurement on XCALIBIR using three DMIs equally spaced around the optical axis.

Keywords:
Radius measurement, Interferometry, Uncertainty

1 INTRODUCTION

Radius of curvature of spherical optical elements is one of the attributes that determines imaging performance and is therefore a key variable in optical system design. If radii deviate from design values, respacing of the elements can provide some compensation, but such 'assembly to wavefront measurement' is costly. Many radius measurement methods are available [1-2], but the radius bench generally gives the lowest uncertainties. However, disagreement between radius bench measurements carried out at different optical shops suggests the need for a better understanding of the measurement model. For example, in a recent round robin of US optics companies [3], the measurement divergence reported for a 100 mm radius test plate was 21 μm or 1 part in 5000, significantly larger than the stated uncertainties (micrometre level).

2 INTERFEROMETRIC RADIUS MEASUREMENT

A radius bench measurement consists of identifying two null positions, confocal and cat's eye, using a figure measuring interferometer (usually a phase measuring interferometer, or PMI) and recording the displacement between the two positions typically using a displacement measuring interferometer, or DMI, aligned with the PMI axis to minimize Abbe error [4]. The confocal null occurs when the curvature of the interferometer spherical wavefront matches the curvature of the test optic surface. Cat's eye is located when the wavefront focus coincides with the part surface, ideally at its center. These null positions give no curvature in the reflected wavefront, i.e., there are no "bulls eye" fringes and, if the wavefront is fit to appropriate orthogonal polynomials (e.g., Zernikes for circular apertures), the coefficient of the quadratic term in radius is zero.

Twyman-Green and Fizeau interferometers may be used, although Fizeau configurations are more common in commercial systems. Radius measurement of a concave spherical surface using a Fizeau is shown in Figure 1 along with the measurand definition used here: the displacement between two positions at which the coefficient for the Zernike power (r^2) term, a_2^0, is zero. These positions are found from the least squares fit to power from multiple phase maps recorded with the part on each side of the confocal and cat's eye nulls.

In this work, radius measurement uncertainty was investigated for measurements on the NIST X-ray Optics Calibration Interferometer (XCALIBIR) of a 25 mm radius polished Zerodur sphere. XCALIBIR is a 300 mm aperture, multipurpose, open architecture PMI that can be configured in either Twyman-Green or Fizeau. The PMI operating wavelength is nominally 633 nm using either a Helium-Neon (He-Ne) laser or diode source. Although not specifically designed for it, XCALIBIR can measure radius by recording the displacement between confocal and cat's eye using three, single pass DMIs. The DMI He-Ne source and three polarization beam splitter/reference retroreflector combinations are fixed to the granite base (4.8 m x 1.5 m x 0.6 m), which also supports the PMI optics. The moving retroreflectors are attached to the 5-DOF mount that carries the test optic. The three DMIs are equally spaced about the PMI optical axis and the recorded displacement is taken to be the average. The uncertainty in the average displacement, and the identification and treatment of correlated versus uncorrelated uncertainty terms, is the focus of this paper. A photograph of the XCALIBIR test setup is shown in Figure 2. Note that the arrangement of the three DMIs yields pitch and yaw, as well as displacement.

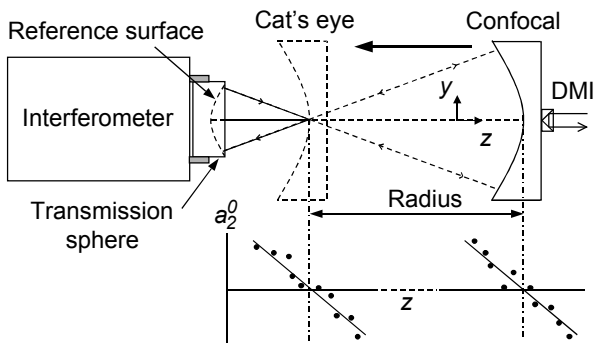

Figure 1: Radius measurement (Fizeau configuration).

XCALIBIR measurements of the Zerodur sphere using Twyman-Green and Fizeau setups at f/numbers ranging from f/1.1 to f/4 have differed by up to 558 nm, although good repeatability (12 nm standard deviation for 12 measurements completed over a one month period) has been demonstrated for a Fizeau f/1.1 transmission sphere setup. An initial uncertainty analysis, using terms available in the literature, predicted a combined standard uncertainty, u_c, of 26 nm [4-5]. Therefore, an expanded uncertainty analysis, which will attempt to better model the measurement, is under development. This analysis

includes the six DMI uncertainties treated in Section 3 plus slide motion and optical (PMI) system uncertainties (e.g., artifact surface figure, null identification, etc.) [6].

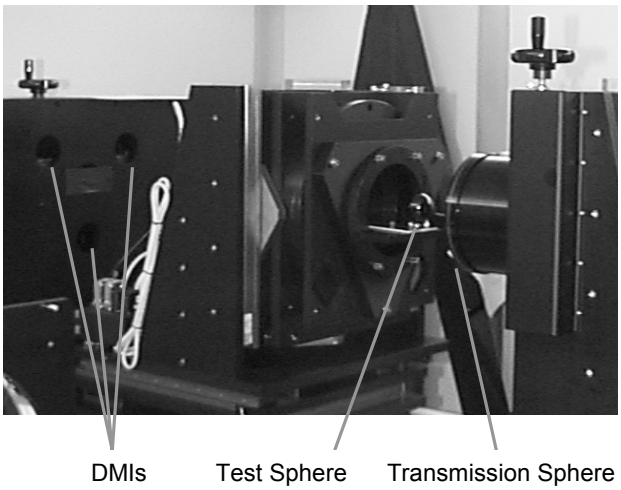

Figure 2: XCALIBIR setup (Fizeau configuration).

Example XCALIBIR measurements of the 24.466 mm radius Zerodur sphere using f/1.1, f/3.2, and f/4 spherical wavefronts with the (one sigma) error bars calculated from the expanded uncertainty analysis [6], as well as the result of a mechanical intercomparison using a Moore-48 CMM (u_c = 50 nm) [7], are shown in Figure 3 (normalized to CMM result). Clearly, all the uncertainty sources have not yet been sufficiently characterized (or not identified) since the error bars do not overlap. The large jumps in the f/4 Twyman-Green measurements occurred after internal realignment of the PMI. Current plans include an evaluation of measurement sensitivity to the PMI setup (e.g., beam expander alignment). However, as previously noted, the purpose of this text is to describe the displacement uncertainty associated with the average value recorded by the three DMIs. Although the magnitude of the individual terms will be specific to XCALIBIR, the analysis can be generalized to treat any situation where multiple DMIs are used to measure displacement in a single axis.

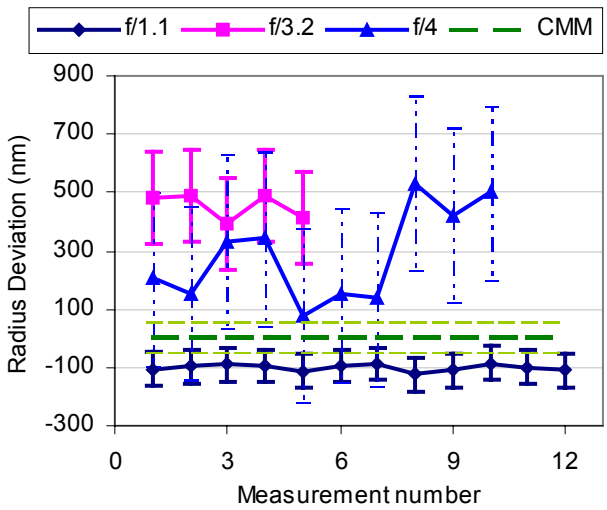

Figure 3: Zerodur sphere measurement results.

3 DMI UNCERTAINTY EVALUATION

Six DMI uncertainty terms (Abbe, cosine, deadpath, environment, turbulence, and laser system) will be described in the following paragraphs. The terms were evaluated using the guidelines found in references [8-9].

3.1 Abbe

The potential for Abbe error exists whenever the measurement axis is not collinear with the quantity being measured. In this case, it occurs if the linear displacement transducer on the radius bench is not collinear with the PMI axis. The relationship between the true and observed displacements, d and d_m, respectively, is shown in Equation 1, where φ is the part rotation relative to the normal to the PMI axis during the measurement and A is the offset between the PMI and displacement measurement axes.

$$d = d_m - A \cdot \tan\varphi \tag{1}$$

The associated uncertainty, u_1, is determined by calculating the 1st-order Taylor series expansion of Equation 1. This result (Equation 2) contains terms which depend on the uncertainties in the best estimate of the observed displacement, $\bar{d}_m$, A, and φ, respectively. The first term is treated by the combination of the six DMI uncertainties, so does not need to be considered separately here. The final term drops out because the expected (or mean) value of A is zero when the three XCALIBIR DMI values are averaged.

$$u_1^2 = u^2(\bar{d}_m) + \tan^2\varphi \cdot u^2(A) + \frac{A^2}{\cos^4\varphi} u^2(\varphi) \tag{2}$$

To quantify the second term in Equation 2, it is necessary to measure the part's angular change between confocal and cat's eye and determine the Abbe offset uncertainty. Pitch, φ_x, and yaw, φ_y, were calculated by differencing the upper/lower and left/right DMI values, respectively, for several measurements. Average values were -30 µrad for pitch and –10 µrad for yaw.

The value for $u(A)$ was determined by simulation. First, the nominal center locations of the three moving retroreflectors were defined. The center of the triangle formed by the nominal retroreflector positions coincides with the motion axis. In MATLAB [7], the retroreflector locations were varied using the uniformly distributed random function, *rand*(N), with an allowable range of +/- 125 µm (from engineering drawings) in x and y. For each set of locations, the triangle center was determined from the intersection point of the two upper angle bisectors (calculated using the point-slope form of the lines). This procedure was repeated many times and the standard deviation in the x and y coordinates of the normalized center locations was 59 µm. Substitution in Equation 2 gives an uncertainty of 2 nm. While small for XCALIBIR, this term can be significant in general. Consider a radius bench with a three-jaw chuck used to hold the optic and a standard linear slide. If the chuck introduces a 2 mm uncertainty in the optic center location and the slide angular uncertainty is 1 mrad, the uncertainty is 2 µm.

3.2 Cosine

Because alignment between the displacement transducer and motion axes cannot be perfectly obtained, cosine uncertainty is inherent to displacement measurement. For DMI measurements, the relationship between the observed and true displacement is given by Equation 3, where β ($0 \le \beta << 1$) is the positive relative angular misalignment between the motion and DMI axes.

$$d = \frac{d_m}{\cos\beta} = d_m \sec\beta \tag{3}$$

While the *most probable* value of β is zero, its *expected* value, $\bar{\beta}$, is a small value of the same order as the uncertainty, $u(\beta)$, to which the DMI beam can be

adjusted parallel to the motion axis. Thus, a reasonable description of what is known about β is that $\bar{\beta} \approx u(\beta)$, which is a small angle on the order of a few arc-sec for a well-aligned system. The uncertainty, u_2, is calculated using Equation 3. Equation 4 gives the full expression, while Equation 5 shows the result of evaluating Equation 4 at the estimate $\bar{\beta} \approx u(\beta) << 1$.

$$u_2^2 = \sec^2\beta \cdot u^2(\bar{d}_m) + \sec^2\beta \tan^2\beta \cdot \bar{d}_m^2 \cdot u^2(\beta) \quad (4)$$

$$u_2^2 = u^2(\bar{d}_m) + \bar{d}_m^2 \cdot u^4(\beta) \quad (5)$$

Because cosine uncertainty gives a single-sided distribution (i.e., the observed displacement is always less than the true displacement in this case), a bias correction must also be applied. This correction is shown in Equation 6, where d_r is the reported value.

$$d_r = \bar{d}_m\left(1 + u^2(\beta)\right) \quad (6)$$

For XCALIBIR, the cosine uncertainty evaluation must include the effect of averaging three DMIs. In this case, u_2 is expressed as shown in Equation 7, where equal alignment uncertainties for each DMI have been assumed. If the first term is again neglected, the resulting uncertainty is 0.1 nm for a radius of 24.466 mm and angular uncertainty of 0.1 mrad. The required bias correction may be calculated using Equation 6.

$$u_2^2 = \frac{1}{3}u^2(\bar{d}_m) + \frac{1}{3}\bar{d}_m^2 \cdot u^4(\beta) \quad (7)$$

3.3 Deadpath

Deadpath error occurs when the DMI measurement and reference path lengths are unequal at initialization and there is an uncompensated change in refractive index, Δn, during the measurement. Fundamentally, this is analogous to changing the measurement starting point. The relationship between the observed and true displacements is given in Equation 8, where L is the difference between the initial DMI path lengths, or deadpath. The associated uncertainty, u_3, is shown in Equation 9, where $u(\Delta n) = u(n_1 - n_2)$ and $n_1 \cong n_2$.

$$d = d_m - \Delta n \cdot L \quad (8)$$

$$u_3^2 = u^2(\bar{d}_m) + L^2u^2(\Delta n) + \Delta n^2u^2(L) = u^2(\bar{d}_m) + 2L^2u^2(n) + \Delta n^2u^2(L) \quad (9)$$

If the refractive index is monitored during the measurement and L is known, a bias correction may be applied to the reported result [10]. This correction is shown in Equation 10. In our case, the temperature, pressure, and relative humidity of the XCALIBIR laboratory were measured to infer index according to Equation 11 [11], where P is air pressure (Pa), T is absolute temperature (K), CO_2 is carbon dioxide content (ppm), and H is relative humidity (% RH).

$$d_r = d_m - \Delta n \cdot L \quad (10)$$

$$n = 1 + 271.8\times10^{-6}\frac{P}{101325}\frac{293.15}{T} \cdot \left(1 + 0.54\left(\frac{CO_2 - 300}{1\times10^6}\right)\right) - 1\times10^{-8}H \quad (11)$$

Averaging the three DMIs leads to the uncertainty expression given in Equation 12, where the following assumptions have been made: 1) deadpaths and deadpath uncertainties are numerically equal, but uncorrelated; 2) index changes and index uncertainties are equal; and 3) uncertainties in displacement best estimates are equal.

$$u_3^2 = \frac{1}{3}u^2(\bar{d}_m) + \frac{2}{3}L^2u^2(n) + \frac{1}{3}\Delta n^2u^2(L) \quad (12)$$

Quantifying this expression requires values for the deadpath, index uncertainty, index change, and deadpath uncertainty. The index uncertainty is obtained from the 1st-order Taylor series expansion of Equation 11 as shown in Equation 13, where the contribution by the uncertainty in air composition has been assumed negligible and the partial derivatives have been evaluated at standard temperature and pressure conditions (20 °C, 101323.2 Pa, and 50% RH).

$$u^2(n) = \left(2.6824\times10^{-9}u(P)\right)^2 + \left(-9.2719\times10^{-7}u(T)\right)^2 + \left(-1\times10^{-8}u(H)\right)^2 \quad (13)$$

For the XCALIBIR laboratory environment, the transducer uncertainty ranges are: ±20 Pa for the barometer (uniform probability distribution), ±0.02°C for the thermistors (normally distributed), and ±2% for the hygrometer (uniform distribution). Substitution of these values into Equation 13 yields the index uncertainty (Equation 14).

$$u^2(n) = \left(2.6824\times10^{-9}\cdot\frac{20}{\sqrt{3}}\right)^2 + \left(-9.2719\times10^{-7}\cdot\frac{0.02}{3}\right)^2 + \left(-1\times10^{-8}\cdot\frac{2}{\sqrt{3}}\right)^2 \quad (14)$$

The expected index change, Δn, was calculated by averaging the change in temperature, pressure, and relative humidity over five arbitrarily selected radius measurements (0.007 °C, 33.6 Pa, and 0.26% RH) and substituting the results in Equation 11 (355 ppm CO_2 assumed). The result was 1 part in 10^7. If the deadpath uncertainty is assumed to have a range of ±3 mm (normally distributed), the resulting uncertainty is 96 nm for a maximum deadpath of 3.5 m (recall that XCALIBIR was not designed to be a radius bench).

3.4 Environment

Environment is similar to deadpath, except the length scale changes with index rather than the starting point. Its treatment is somewhat different, however. In the case of deadpath, it is reasonable to assume the three deadpath lengths are uncorrelated (even though they have been taken to be numerically equal). In the case of environment, there is only one value for index change so no new information is gained by averaging because the three measurements are correlated (through index).

Care must still be exercised with environment uncertainty evaluation, however, because the difference between the true and observed displacement (an optical path difference) is the product of the change in index and actual physical displacement, D (nominally equal to the radius for the largest probable error during motion from confocal to cat's eye). The measurement model and corresponding uncertainty are given in Equations 15 and 16.

$$d = d_m - \Delta n \cdot D \quad (15)$$

$$u_4^2 = u^2(\bar{d}_m) + 2D^2u^2(n) + \Delta n^2u^2(D) \quad (16)$$

The final term in Equation 16 contains the uncertainty in D. This represents the 'counting' uncertainty in the DMI phase measuring electronics since initialization. The value of the DMI resolution (0.62 nm) has been selected

for this uncertainty term. Neglecting the first term in Equation 16 and using the previous values for radius (D = 24.466 mm), index uncertainty, and index change gives an uncertainty of 0.7 nm.

3.5 Turbulence

Optical path difference due to air turbulence in the environment has been investigated [10, 12]. Typical airflow velocities in temperature-controlled environments affect the refractive index of air through time-dependent thermal and pressure fluctuations. Specifically, 1) the low thermal diffusivity of air causes thermal inhomogeneities to be mixed before they can come to equilibrium, and 2) turbulent airflow can cause local pressure fluctuations. The correlation coefficient (due to turbulence) between two paths depends on their separation and the air velocity. XCALIBIR has an airflow velocity of ~10 m/min with a path separation of 204 mm, so it is reasonable to assume a worst case correlation coefficient of unity [12]. Therefore, averaging will not reduce the uncertainty. The range in values for a single DMI channel recorded over a short time scale is ±6 nm. If a normal distribution (with a 2 out of 3 chance that the recorded range bounds the data) is assumed, the resulting uncertainty is 3 nm.

3.6 Laser System

The components of the heterodyne laser system that affect the uncertainty are laser wavelength stability, polarization characteristics of the laser beam, interferometer errors from two sources (polarization mixing and thermal effects), and electronics linearity. The manufacturer-specified values for the system used in this research are ±10 nm/m, ±0.8 nm, ±0.8 nm, 22 nm/°C, and ±0.8 nm, respectively. Also considered here is the frequency mixing, and resulting periodic error, that results from imperfect alignment between the optical axes of the polarization-coded two-frequency light and the polarization beam splitter. A range of ±2 nm is assumed. The treatment of each uncertainty source for the XCALIBIR setup follows.

Since there is a single He-Ne source, wavelength stability uncertainty and beam polarization characteristics between channels are correlated. Interferometer errors and electronics linearity can be considered uncorrelated because there are three separate interferometers and measurement boards. Periodic error is also uncorrelated because each of the interferometers is aligned independently. These six uncertainty sources are combined in Equation 17, where a uniform distribution for each uncertainty source (except temperature which is treated as normally distributed) has been assumed. Also, uncorrelated terms have been divided by three to account for the reduction in uncertainty due to averaging. If a temperature range of 0.02 °C and nominal radius of 24.466 mm are inserted, the resulting uncertainty from Equation 17 is 0.9 nm.

$$u_6{}^2 = \left(\frac{10}{\sqrt{3}}0.024466\right)^2 + \left(\frac{0.8}{\sqrt{3}}\right)^2 + \frac{1}{3}\left(\frac{0.8}{\sqrt{3}}\right)^2 + \frac{1}{3}\left(22\frac{0.02}{3}\right)^2 + \frac{1}{3}\left(\frac{0.8}{\sqrt{3}}\right)^2 + \frac{1}{3}\left(\frac{2}{\sqrt{3}}\right)^2 \quad (17)$$

3.7 DMI Combined Standard Uncertainty

The uncertainty contribution of the DMIs to the overall measurement uncertainty of the Zerodur sphere on XCALIBIR is calculated by summing in quadrature the six terms quantified in the previous paragraphs. The result is 96 nm. Clearly the uncertainty is driven by the deadpath (the maximum deadpath of 3.5 m has again been assumed). In the XCALIBIR design, deadpath varies with setup (smaller uncertainty for Fizeau f/1.1 and larger uncertainty for Twyman-Green f/4, as seen in Figure 3). Mechanical changes could be made to eliminate or minimize the problem [6].

4 CONCLUSIONS

A description of the uncertainty terms that occur when using multiple displacement measuring interferometers (DMIs) to record displacement along a single axis, as well as the logic used to discern between correlated and uncorrelated uncertainties, has been provided. The uncertainty terms have been quantified for radius of curvature measurements of a 24.466 mm radius polished Zerodur sphere performed on the NIST X-ray Optics Calibration Interferometer (XCALIBIR). In this setup, three DMIs are equally spaced around the motion axis. The average value is reported as the observed displacement, while differencing individual values gives pitch and yaw information. The dominant uncertainty term was deadpath (range was 27 nm to 96 nm for data reported here). However, the potential for a larger uncertainty when using typical radius benches due to uncertainty in Abbe offset (even if the displacement transducer is nominally in line with the part axis) was described. Future measurements aimed at isolating radius error sources and providing full overlap of the calculated uncertainties were also covered.

5 ACKNOWLEDEMENTS

The authors would like to thank T. Doiron and J. Stoup, NIST, for performing the mechanical measurements of the Zerodur sphere.

6 REFERENCES

[1] Malacara, D., 1992, Optical Shop Testing, John Wiley & Sons, New York.

[2] Murty, M., Shukla, R., 1983, Measurements of long radius of curvature, Optical Engineering, 22:231-235.

[3] Sponsored by Plympton, R., Optimax Systems, Inc., Ontario, NY.

[4] Selberg, L., 1992, Radius measurement by interferometry, Optical Engineering, 31:1961-1966.

[5] Schmitz, T., Evans, C., Davies, A., 2000, An investigation of uncertainties limiting radius measurement performance, Proceedings of ASPE Spring Topical Meeting, Tucson, AZ, May 10-12, p. 27.

[6] Schmitz, T., Davies, A., Evans, C., 2001, Uncertainties in interferometric measurements of radius of curvature, Optical Manufacturing and Testing IV, Stahl, H. P., Editor, Proceedings of SPIE, 4451:432-447.

[7] Commercial equipment identification does not imply endorsement by NIST.

[8] International Organization for Standardization (ISO), 1995, "Guide to the Expression of Uncertainty in Measurement," Geneva.

[9] Taylor, B., Kuyatt, C., 1994, NIST Technical Note 1297, Guidelines for Evaluating and Expressing the Uncertainty of NIST Measurement Results.

[10] Estler, W. T., 1985, High-accuracy displacement interferometry in air, Applied Optics, 24:808-815.

[11] Bobroff, N., 1993, Recent advances in displacement measuring interferometry, Measurement Science and Technology, 4:907-926.

[12] Bobroff, N., 1987, Residual errors in laser interferometry from air turbulence and nonlinearity, Applied Optics, 26:2676-2682.